ELSEVIER

Contents lists available at ScienceDirect

Developments in the Built Environment

journal homepage: www.sciencedirect.com/journal/developments-in-the-built-environment



Use of bio-waste for silica aerogel composites

Samuel Pantaleo *0, Fenne Adriaanse, Florent Gauvin, H.J.H. Brouwers

Department of the Built Environment, Vertigo, PO BOX 513, 5600 MB, Eindhoven, the Netherlands

ARTICLE INFO

Keywords:
Building performance
Silica-aerogel
Thermal conductivity
Bio-sourced waste materials
Innovative building materials

ABSTRACT

Silica aerogel, with its exceptionally low thermal conductivity, needs wider applications despite current limitations. Meanwhile, bio-sourced materials are gaining traction because of their large availability, with comparable or superior properties to non-renewable options. Additonnaly, their low carbon footprints are crucial for reducing emissions linked to the building sector. Therefore, combining silica aerogel with bio-sourced materials is a promising way to address both environmental and performance goals. In the present study, composites made of silica aerogel and bio-based materials issued from waste (e.g. loose cellulose fibers and sawdust) are investigated, aiming for thermal insulation as the main application. The impact of each component is studied on properties related to thermal insulation - thermal conductivity, mechanical strength, moisture behavior, and mold development. Using empirical methodology, fine-tuned compositions are developed to get the best properties. Thermal conductivity down to 20 mW m⁻¹.K⁻¹ is achieved, with compression strength fulfilling the standard for thermal insulation materials.

1. Introduction

Global warming, driven principally by the increase in greenhouse gas (GHG), is a pressing issue causing higher temperatures and poses severe risks for the coming years. The energy sector contributes significantly to GHG, accounting for 34 % of the total emissions (United Nations Environment Programme, 2022), with around 25 % of the energy used for heating and cooling buildings. Therefore, developing improved thermal insulation materials is crucial for reducing these GHG emissions. Moreover, beside the operational energy, the material footprint itself is another large contributor to GHG emissions, accounting for 37 % of GHG (Iea). Improving the sustainability of insulation, without compromising on the insulation capacity, is therefore crucial in the building sector.

There are many good candidates for improving building insulation, with a lot of recent research focusing on the development of new materials, with better overall performances. Among them, Silica aerogel is an outstanding thermal insulator, made of a 3-dimensional Si-O-Si network with 95–98 % of air. Silica aerogel is flame-retardant (Yu et al., 2018), lightweight, and has a thermal conductivity lower than most of the thermal insulators available on the market, ranging from 12 to 20 mW m $^{-1}$.K $^{-1}$ (Koebel et al., 2012), and is currently one of the best-performing thermal insulations available, as shown in Table 1.

Silica aerogel is available in various forms depending on its size, allowing for a wide range of applications. It is used in drug delivery (Soghra et al.), fiber coatings (Soghra et al.), and thin films (Lin et al., 2023) in its powder form, and as building materials as cement fillers (Berardi and Nosrati, 2018) or window glazing (Bin Rashid et al., 2023), and also as reinforced thermal insulation when in granulate form. However, silica aerogel has some key drawbacks: it is expensive, naturally brittle, and its production requires significant energy. To overcome these issues and continue the development of silica aerogel applications, adding a reinforcement is a promising approach. In the literature, two main strategies can be observed: The first approach is to strengthen the silica network itself via chemical modification or by adding fibers. Reinforcement of silica aerogel during its synthesis is already successfully achieved (Yu et al., 2018), (Yang et al., 2023), (Rong et al., 2013), (Zhang et al., 2023), (Zhang et al., 2020) while maintaining a low thermal conductivity. The second approach involves mixing silica aerogel and a binder (Zhang et al., 2023), (Brouwers), (Kucharek et al., 2020). However, all these strategies are using fossil-based materials, which would be preferable to avoid to reduce the carbon footprint of the composite. Bio-based materials offer promising alternatives to fossil-based materials due to their ease of production, abundant sources (150 million tons (Faruk et al., 2012)), growing availability from waste, and good mechanical properties. They are mainly used as reinforcements in plastic or inorganic composites but can also be used as binders (Musco et al., 2024).

For thermal insulation applications, bio-based materials are already

E-mail address: s.m.pantaleo@tue.nl (S. Pantaleo).

^{*} Corresponding author.

Table 1Thermal conductivity of typical thermal insulation materials.

Insulation materials	Density (g.cm ⁻³)	Thermal conductivity (mW.m $^{-1}$. K^{-1})
Hemp	0.038-0.041 (Grazieschi et al., 2021)	65 (Koh et al., 2022)
Cork	0.160–0.240 (Ijjada and Nayaka, 2022)	49–50 (Ijjada and Nayaka, 2022)
Cellulose	0.034–0.044 (Ijjada and Nayaka, 2022)	40 (Ijjada and Nayaka, 2022)
Mineral wool	0.035–0.130 (Grazieschi et al., 2021)	35–65 (Koebel et al., 2012), (Ijjada and Nayaka, 2022)
Polystyrene	0.009-0.030 (Liu et al., 2019a)	29–55 (Koebel et al., 2012)
Polyurethane	0.030-0.200 (Demharter, 1998)	20-29 (Koebel et al., 2012)
Silica aerogel	0.008-0.020 (Koebel et al., 2012)	12-25 (Koebel et al., 2017)

used in several products, but their thermal conductivity, usually quite low as they are intrinsically porous, struggles to reach a value of 35 mW $\rm m^{-1}.K^{-1}$ or lower. Therefore, these materials cannot be considered ultralow thermal insulators, limiting their development as next-generation thermal insulators. Some examples, with a very broad range of thermal conductivities, as displayed in Table 2.

Achieving very low thermal conductivity (i.e., below 30 mW m $^{-1}$. K⁻¹) with bio-based materials is quite challenging, and therefore, different strategies need to be investigated. Among the available options, using biobased material together with silica aerogel is seen as promising: Indeed, the addition of silica aerogel to a bio-based binder could improve thermal insulation efficiency while using a significant amount of bio-based materials. Only few works investigated the combination of bio-based materials and silica aerogel, and they rely most of the time on a synthesis to combine these two materials (Sarkar et al., 2024), (Wang et al., 2024). This work is using raw materials, with a straight forward process. Besides thermal insulation, other factors need to be considered, such as moisture absorption and the possible impact on thermal conductivity (Koh et al., 2022), adhesion between bio-based components and silica aerogel, ensuring minimum strength for handling and installation, and addressing potential mold development on bio-based materials (Koh et al., 2022), (Koh et al., 2023). The contribution of each component of the composite to the thermal conductivity needs to be investigated and understood to further fine-tune and optimize the mix composition based on the targeted properties or

In this work, waste-based materials such as loose cellulose fibers from paper recycling and sawdust are mixed with silica aerogel granulates, using a bio-based binder (e.g. xanthan gum and glycerol) resulting in a composite material, that can be used as building insulation. The contribution of each component is assessed, as well as other important properties, such as compressive strength, fire resistance, or mold development.

 Table 2

 Thermal conductivity values of bio-based materials.

Insulation materials	Thermal conductivity (mW. m^{-1} . K^{-1})	Ref.
Wheat straw insulation panel	92–186	Liu et al. (2019b)
Mycobam (Bamboo + Mycelium)	80	Carcassi et al. (2022)
Cork fiber Gypsum 60/40	62.3	Sair et al. (2019)
Insulation Corkboard	40	Cosentino et al. (2023)
Sheep wool loose-fill fibers	35	Parlato et al. (2022)

2. Materials and methods

2.1. Materials

Silica aerogel granulates are obtained from Cabot Corporation, USA (Aerogel Particles P100® – Size from 0.1 to 4.0 mm). Xanthan Gum (Analytical grade) and Glycerol (Analytical grade) are purchased from VWR Chemical, the Netherlands. Cellulose (Cyclin® Cellulose Sound Insulation) is purchased from De Isolatieshop B.V., the Netherlands, and blended to obtain loose cellulose (inhomogeneous). Sawdust (size range: $500{-}1200~\mu m$) is purchased from La.So.Le. Est, Italy.

2.2. Thermal gravitational analysis - TGA

Thermal gravitational analysis (TGA) is performed using a TG 209F3 NETZSCH® to investigate the thermal stability of the different compositions. The analysis is done from 30 °C to 900 °C at 10 °C.min $^{-1}$. The stability of the samples is assessed by looking at the mass changes due to temperature increases and product evaporation. Samples are dried at 50 °C overnight before analysis. Samples of 20 mg are measured.

2.3. Moisture sorption

Moisture uptakes of the samples are measured in several relative humidity (RH) conditions using saturated salt solutions, i.e., magnesium chloride hexahydrate (MgCl $_2$.6H $_2$ O) for 33 % RH, potassium carbonate (K $_2$ CO $_3$) for 43 % RH, sodium chloride (NaCl) for 75 % RH, and potassium chloride (KCl) for 85 % RH. Before analysis, samples are dried overnight at 40 °C (Memmert universal oven UF260). For each RH, samples are left in the desiccator for at least 48 h before the first measurement. After that period, measurements are taken every 24 h for a week.

$$WU = \frac{m_{\rm x} - m_{\rm 0}}{m_{\rm 0}} \pm 100 \tag{1}$$

Where m_x stands for the mass at different times, m_0 stands for the initial mass, and WU for water uptake.

Weight measurements are taken at room temperature (20 \pm 2 $^{\circ}$ C).

2.4. Thermal conductivity

The transient plane source method is used for the measurement of thermal conductivity λ (mW.m $^{-1}$ K $^{-1}$), using a Hot Disk Thermal Constants Analyser (TPS 2500 S) equipped with a 5501 r2 sensor at room temperature (20 \pm 2 °C), with a declared accuracy of 5 % of the reading plus 0.1 mW m $^{-1}$.K $^{-1}$. The Hot Disk is calibrated (Malfait et al., 2024) with an EPS sample provided by the manufacturer, with a declared thermal conductivity of 25.3 mW m $^{-1}$.K $^{-1}$. Samples from the procedure described above are tested, and λ values are determined. A minimum of 6 measurements are made to minimize the error. Before the measurement, the samples are dried at 50 °C in an oven (Memmert universal oven UF260) to remove a maximum of water or conditioned in desiccators at various relative humidities (33 %, 43 %, 53 %, 75 %, 85 %, and 98 %), to assess the impact of moisture on the thermal conductivity.

2.5. Bulk density

The bulk density is determined using Equation (3).

$$\rho_{bulk} (g / cm3) = \frac{Mass (g)}{Volume (cm^3)}$$

Within formula, the mass (g) is determined on dried samples (40 °C, overnight) using a gravimetric scale, while the sample volume (cm³) is determined using calipers.

2.6. Dynamic vapor sorption - DVS

Sorption isotherms of the composites are measured using the gravimetric sorption technique through dynamic vapor sorption (DVS) (Surface Measurement Systems DVS Resolution). The specimen is conditioned in a relative humidity RH environment between 0 % and 95 % RH. The weight of the specimen is measured at a 10 % RH increment step for the sorption curve, and at a 10 % decrement step for the desorption curve, all under a constant temperature of 20 °C. The specimen is considered to reach its constant mass once the rate of mass change dw/dt (%kg.kg1.min $^{-1}$) is equal to or less than 0.01. The DVS apparatus has a declared accuracy of 0.5 % RH reading.

2.7. Compression tests

Mechanical strengths of the composite latex/silica aerogel are tested through compression tests, using an MTS Criterion equipped with a 30 kN load cell, at a test speed of 2 mm/min, and room temperature. A minimum of 5 samples (30 mm * 30 mm * 10 mm – BS EN 826) are tested for every condition.

2.8. Scanning electron microscopy - SEM

Analyses are performed using a Phenom Pro-X microscope (Thermo Fisher Scientific). Observations are done at different voltages and magnifications, with a backscattered electron detector. Samples are gold-coated (Quorum Q150T Plus – 30 mA, coating time = 30 s) before analysis.

2.9. Flame retardancy

Flame retardancy tests are conducted, derived from standard UL 94. Samples (30 mm * 30 mm * 10 mm) are exposed for 10 s to a flame coming from a Bunsen burner, at a 45° angle, placed 20 mm away from the sample. 3 samples are tested per condition. After and if the flame is resorbed, samples are exposed to the flame a second time, with the same conditions, at the same spot. The final aspect of the sample and the burning time are recorded.

2.10. Mold development

Mold development assessments are done by placing samples in a desiccator at 98 % RH (K_2SO_4) for 14 and 28 days. Raw components, composites, and binder are tested, and pictures of before and after are taken to assess and compare the mold development.

2.11. Sample design

The slurry investigated by Rech et al. (2022), using water, xanthan gum, and glycerol, is used as reference for this study. After mixing with a high-speed mixer, loose cellulose fibers (CI) and sawdust (SD) are added as reinforcement. From that starting material, silica aerogel (SA) is added to enhance the thermal insulation. It is added as a replacement for the two other fillers to keep the final weight percentages of fillers at 18 wt%, as illustrated in Fig. 1.

Table 3 summarizes the different mix design for this study. Firstly, samples composed only of one of the components are made. Then, samples with silica aerogel are made, with a gradual increase in the amount of silica aerogel in the mix. The amount of SD and CI decreases to always keep the filler amount at 18 wt%.

Samples (30 \times 30 \times 30 mm) of the different mixes, shaped with a 3D printed mold, can be seen in Fig. 2. All the compositions have enough viscosity to be molded and can keep their shape during drying. Samples are dried in an oven (50 $^{\circ}$ C, overnight).

Shrinkage can be observed after drying the samples, as seen in a previous study from Rech et al. (2022), even with the addition of silica aerogel, though it helps decreasing the shrinkage. From condition A5.0, no noticeable shrinkage can be observed after drying. Later on, samples with optimized conditions are prepared to emphasize the contribution of each filler to the thermal conductivity of the composites. The amount of one of the bio-based fillers is lowered, while its counterpart is kept constant. The first round of optimized conditions can be seen in Table 4.

Fig. 3 displays the samples after oven drying. Similar to the first trials, a small shrinkage is observed for the compositions with 2.5 wt% of silica aerogel.

Lastly, and based on the first thermal conductivity measurements (see Fig. 8), sawdust is completely removed from the composition, and the amounts of cellulose fibers and silica aerogel are fine-tuned to enhance as much as possible both thermal insulation and physical properties. Filler amounts remain at 18 wt% of the total mix, and compositions are listed in Table 5.

Fig. 4 displays the samples after oven drying. Similar to the first trials, a small shrinkage is observed for the compositions with 2.5 wt% of silica aerogel.

Similar to the first batch of samples, shrinkage can be observed for the samples with a silica aerogel amount below 5 wt%.

3. Results and discussions

3.1. Thermal analysis

Thermal gravitational analysis is performed on the raw samples and

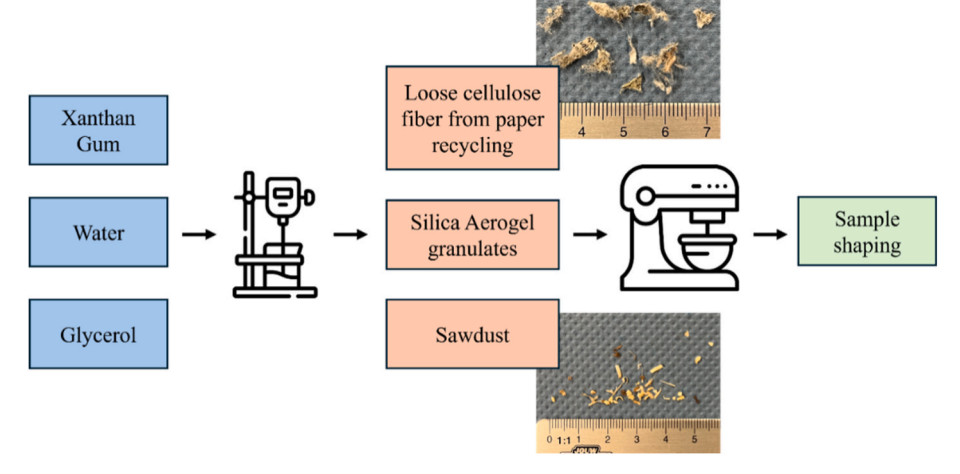


Fig. 1. Illustration of the process of silica-aerogel/bio-based materials.

Table 3
Names and compositions of the early tests of silica aerogel/bio-based materials composites – "A2.5" standing for 2.5 wt% Silica Aerogel.

Sample Name	Water (wt%)	Xanthan Gum (wt%)	Glycerol (wt%)	Loose Cellulose Fiber (wt%)	Sawdust (wt%)	Silica aerogel granulates (wt%)
SD	72.0	2.0	8.0	0.0	18.0	0.00
CI	72.0	2.0	8.0	18.0	0.0	0.0
Ref	72.0	2.0	8.0	10.5	7.50	0.0
A2.5	72.0	2.0	8.0	9.25	6.25	2.5
A5.0	72.0	2.0	8.0	8.0	5.0	5.0
A7.5	72.0	2.0	8.0	6.75	3.75	7.5
A10.0	72.0	2.0	8.0	5.5	2.5	10.0
A18.0	72.0	2.0	8.0	0.0	0.0	18.0

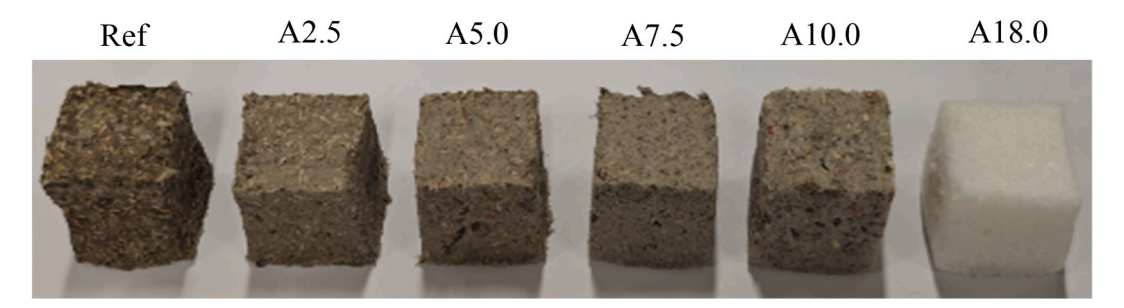


Fig. 2. Dried samples of early tests of silica aerogel/bio-based materials composites.

Table 4

Names and compositions of the optimized compositions of silica aerogel/bio-based materials composites – "A2.5-R-CI" standing for 2.5 %wt Silica aerogel, with a reduced amount of Cellulose Fiber.

Sample Name	Water (wt%)	Xanthan Gum (wt%)	Glycerol (wt%)	Loose Cellulose Fiber (wt%)	Sawdust (wt%)	Silica aerogel granulates (wt%)
A2.5-R-CI	72.0	2.0	8.0	8	7.5	2.5
A5.0-R-CI	72.0	2.0	8.0	5.5	7.5	5.0
A7.5-R-CI	72.0	2.0	8.0	3.0	7.5	7.5
A2.5-R-SD	72.0	2.0	8.0	10.5	5.0	2.5
A5.0-R-SD	72.0	2.0	8.0	10.5	2.5	5.0
A7.5-R-SD	72.0	2.0	8.0	10.5	0.0	7.5

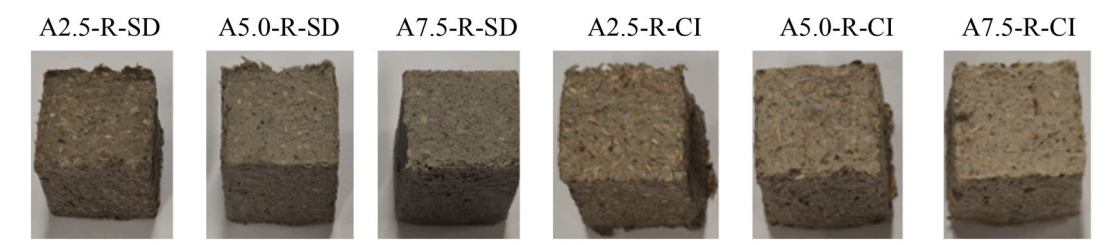


Fig. 3. Dried samples of the optimized composition of silica aerogel/bio-based materials composites.

 Table 5

 Names and compositions of the optimized compositions of silica aerogel/bio-based materials composites – "SA-CI-3" standing for 3 wt% of cellulose fibers.

Sample Name	Water (wt%)	Xanthan Gum (wt%)	Glycerol (wt%)	Loose Cellulose Fiber (wt%)	Sawdust (wt%)	Silica aerogel granulates (wt%)
SA-CI-3	72.0	2.0	8.0	3.0	0.0	15.0
SA-CI-4	72.0	2.0	8.0	4.0	0.0	14.0
SA-CI-5	72.0	2.0	8.0	5.0	0.0	13.0

the different composites to assess the potential effect of the binder on the decomposition temperature. TGA curves for the raw materials and the binder are displayed in Fig. 5.

Firstly, all the samples exhibit a small mass drop of \sim 5 wt%, corresponding to trapped moisture in the sample. Due to the high hydrophilicity of the components, the complete drying of the sample is not possible to achieve. TGA on the raw cellulose showcases two main products: cellulose, with the \sim 350 °C peak ((Chen et al., 2019), (Zhang

et al., 2012)), and lignin, with several small decomposition peaks over the whole TGA run, highlighted with characteristic \sim 500 °C and \sim 750 °C peaks ((Chen et al., 2019), (Zhang et al., 2012)). On the other hand, only one peak is observed for the sawdust at 350 °C. When combined with the binder, both materials exhibit a new decomposition peak at \sim 200 °C, attributed to the glycerol decomposition (Benitez et al., 2024). The mass loss observed for these picks corresponds to the expected dry amount of glycerol (28 wt%) of the initial 28 wt% of solid

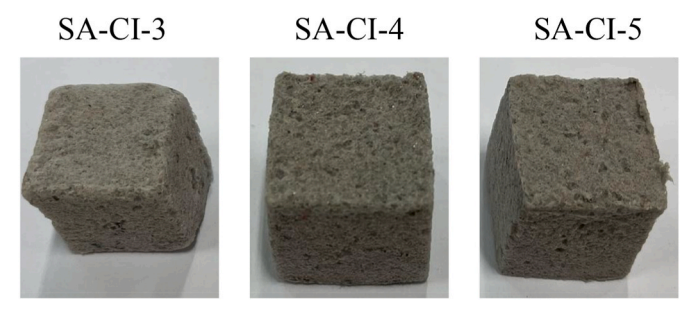


Fig. 4. Dried samples of the optimized composition of silica aerogel/bio-based materials composites.

fraction. Considering the xanthan gum, its decomposition temperature occurs at around 290 °C (Faria et al., 2011), resulting in the small shifts on the TGA curves, but its small quantity combined with a decomposition temperature close to the cellulose makes it difficult to clearly identify it on the DTG curves. The binder addition does not affect the decomposition of either the cellulose or the sawdust. Following this, TGA runs are performed on the different mixes prepared, either on the simple or optimized ones. Fig. 6 displays the TGA/DTG curves of several samples, and the decomposition temperatures with the associated mass losses are reported in Table 6.

Similar to the raw materials, no shifts in temperature decomposition are observed in the TGAs. The same weight drops relative to water evaporation, already observed on the raw components' TGA, are also observed here, and so will not be tracked. The final masses follow the amount of silica aerogel in the composites, and the binder does not affect the temperature decompositions (Table 6).

As seen for the first composites, weight losses regarding glycerol are identified, around $\sim\!200$ °C, with corresponding mass loss. The final mass also follows the amount of silica aerogel added. Among the last batch of samples, the mass losses and the decomposition temperature attributed to the first degradation differ among the samples. Yet, this effect is explained by the lack of homogeneity of the samples, due to their small quantity in the TGA pan. As seen in Fig. 7, displaying retakes of the A5.0-R-CI samples, shifts regarding the onset around 200 °C are observed, in a range of approximately 20 °C.

These small shifts around 200 $^{\circ}$ C are observed for the majority of the samples. Based on these results, TGA analysis shows that the mixing of all these components does not interfere with their thermal behavior.

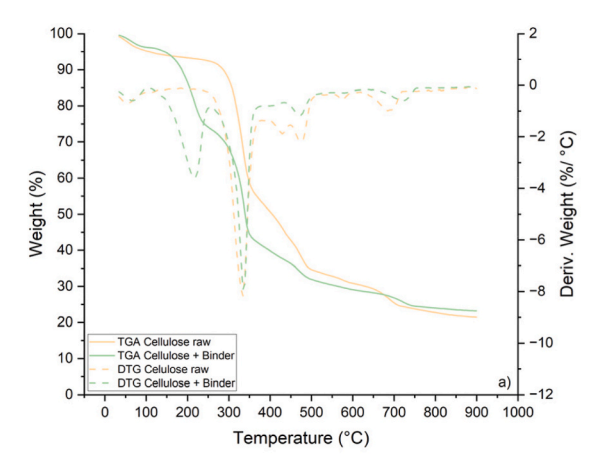
3.2. Thermal conductivity

Thermal conductivity of the raw material alone, raw materials with the binder, the first silica aerogel mixes, and the optimized compositions are measured. Results are displayed in Fig. 8.

Firstly, it can be observed that the pure samples made with one component and the binder exhibit a thermal conductivity way higher than their components alone (61 mW m⁻¹.K⁻¹ and 57 mW m⁻¹.K⁻¹ versus 91 mW m $^{-1}$.K $^{-1}$ and 131 mW m $^{-1}$.K $^{-1}$ – Fig. 8-a). This results is expected as the thermal conductivity of the binder is quite high 297.5 mW m⁻¹.K⁻¹. The same behavior is observed for the reference samples (Ref.), with a maximum of 127 mW m⁻¹.K⁻¹. All these rises in thermal conductivity can be attributed to the binder (Binder XG), which exhibits alone a thermal conductivity of 297.5 mW m⁻¹.K⁻¹. It is important to note that no difference can be observed between the samples composed of silica aerogel, with (A18.0) or without a binder (SA Raw). Looking at the composites, adding silica aerogel proportionally lowers the thermal conductivity of the samples. An important decrease in thermal conductivity is observed, from 127 mW m⁻¹.K⁻¹ without silica aerogel (Ref.) to 40 mW m⁻¹.K⁻¹ for the highest silica aerogel amount with biobased material (A10.0 - Fig. 8-b). It shows that a significant amount of silica aerogel needs to be added to the composite to have an important impact on the thermal conductivity. Yet, for the best composition, 40 mW m⁻¹.K⁻¹ is reached, but remains quite high, and fine-tuning of the composition is needed to reduce it more.

Fig. 9-a) displays the thermal conductivity of the composites made with a reduction of either Sawdust (SD) or Cellulose (CI), aiming to reach lower thermal conductivities.

All the trials show a small decrease in thermal conductivity, compared to their equivalent with the initial compositions ($\lambda_{A~2.5}=106$ mW m⁻¹.K⁻¹ vs $\lambda_{A 2.5-R-CL} = 87.2$ mW m⁻¹.K⁻¹), but none of them are able to reach a thermal conductivity low enough, with the lowest thermal conductivity achieved at 43.7 mW m⁻¹.K⁻¹. The starting point of the last composition is the one without any bio-based materials. Small amounts of Cellulose insulation are added to the mix (3, 4, and 5 wt%), and the results showcase a real drop in thermal conductivity, with a minimum value at 19.7 mW m⁻¹.K⁻¹ (Fig. 9-b). Even for these small differences in cellulose amount, a noticeable change among the samples can be observed, with a difference up to 10 mW m⁻¹.K⁻¹ between 3 wt% and 5 wt%. Looking at the results, bio-based fibers have an important impact on the thermal conductivity of the composites. This is explained by the important gap in thermal insulation capacity between them and silica aerogel. In addition, mixing silica aerogel with other materials, not matter their insulation capacity, limits its efficiency by increasing the heterogeneity in the materials, leading to reduced radiative conductivity but increased conductive conductivity, which result in an increase of the thermal conductivity (Xie et al., 2013). In our study, cellulose fiber can still be used while keeping a good thermal insulation capacity. The density of the Ref. sample and most optimized composition is measured and compared to typical insulation materials, Hemp, Cellulose, Polystyrene and Cork (Table 1). Results are displayed in Fig. 10.



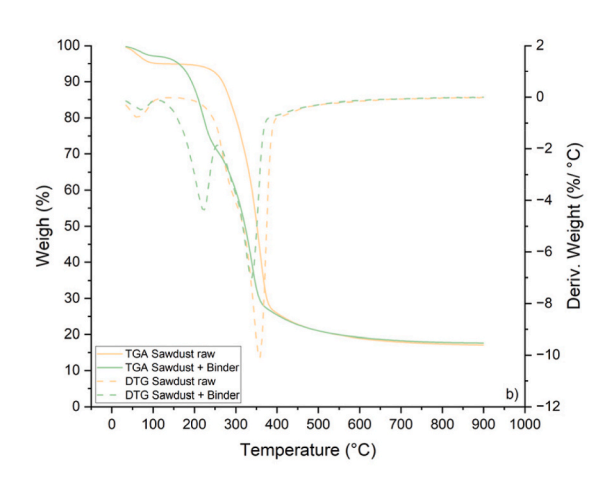


Fig. 5. TGA and DTG curves of raw materials: a) Cellulose insulation, b) Sawdust.

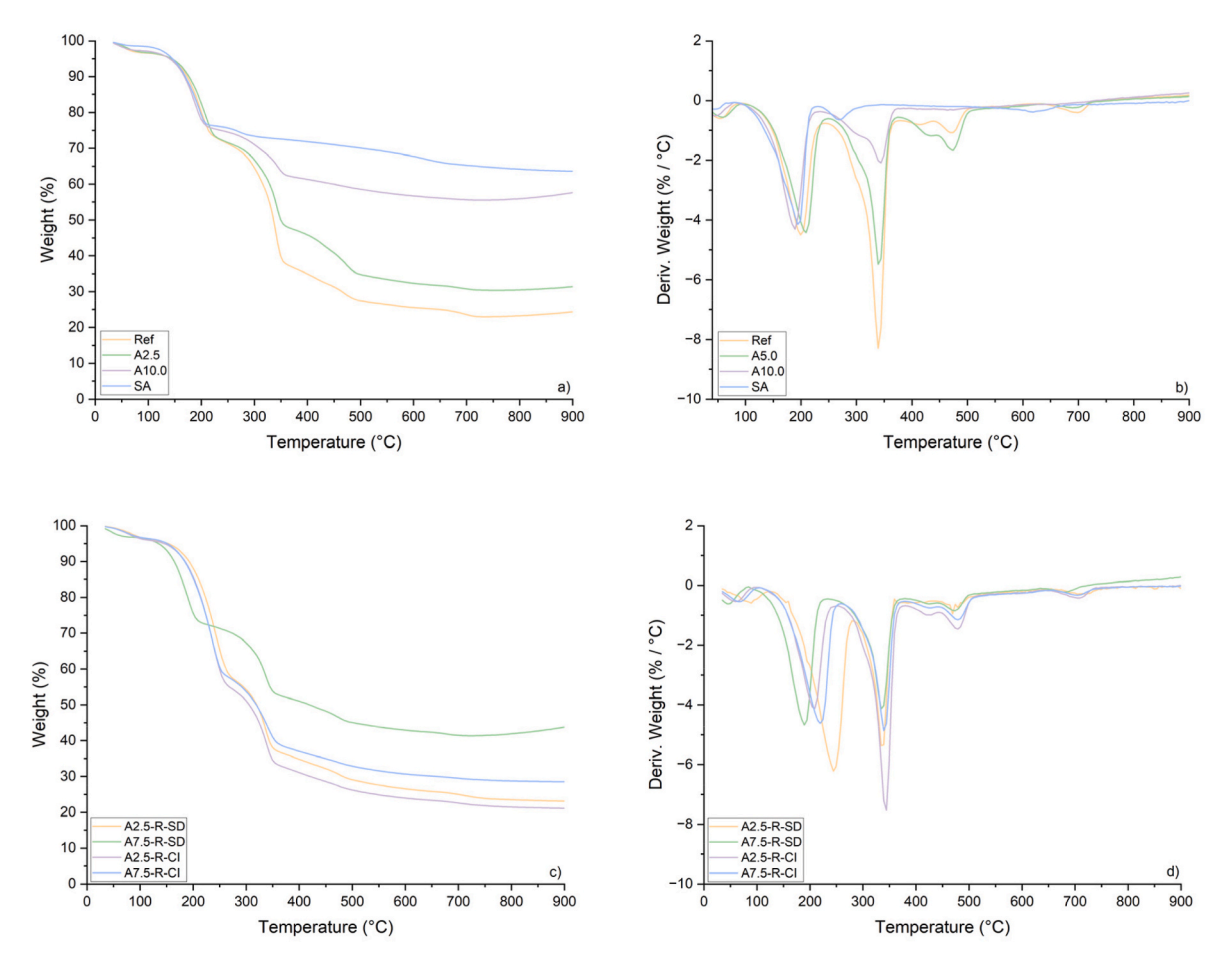


Fig. 6. TGA and DTG curves of composites: Early trials a) and b) - Optimized compositions c) and d).

Decomposition peaks of the different TGA.

Name	1st degradation		2nd degradation		3rd degradation		Final
	Temp. (°C)	Mass loss (%)	Temp. (°C)	Mass loss (%)	Temp. (°C)	Mass loss (%)	mass (%)
Ref	200	24	340	35	470 + 700	9 + 2	22
A2.5	209	23	340	22	475 + 695	11 + 2	30
A10.0	195	25	345	13	ε	ε	62
A18.0	189	22	260	2	ε	ε	70
A2.5- R- SD	244	36	339	19	469 + 720	6 + 2	22
A7.5- R- SD	189	25	334	20	474 + 680	5 + 2	41
A2.5- R-CI	204	43	344	21	479 + 704	3+2	20
A7.5- R-CI	219	39	340	20	479 + 704	5 + 0	28

The addition of silica aerogel significantly reduces the material's density. A minimum value of $0.147~g~cm^{-3}$ is reached in the composition with the lowest thermal conductivity, compared to $0.345~g~cm^{-3}$ for the initial material. The optimized composition falls within this range. Although this density is relatively high compared to conventional insulation materials, the designed material still exhibits thermal

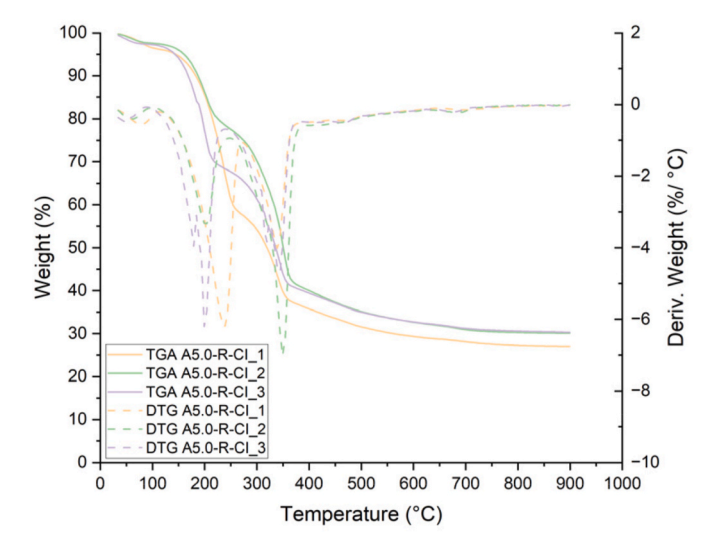
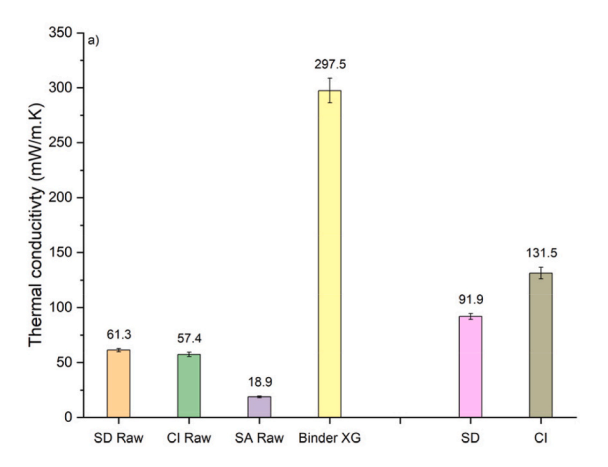


Fig. 7. TGA and DTG curves of composites. Comparison of retakes of A5.0-R-CI.

conductivities that are comparable to, or even lower than, those of such insulators. Moreover, the higher density may contribute positively to the mechanical performance of the sample.

3.3. Mechanical properties

The different compositions are tested under compressive testing to



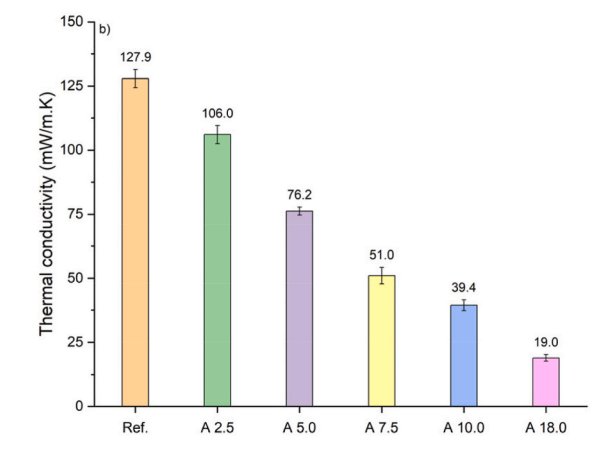
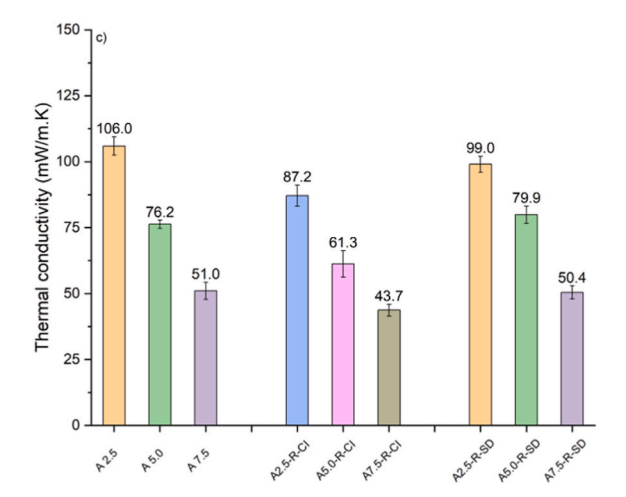


Fig. 8. Thermal conductivity of the different compositions: a) Raw materials, b) First trials.



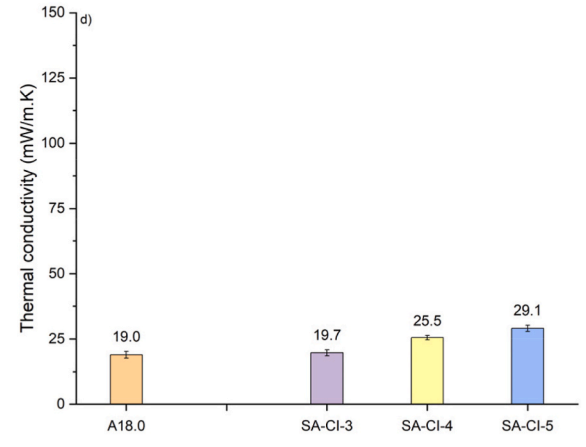
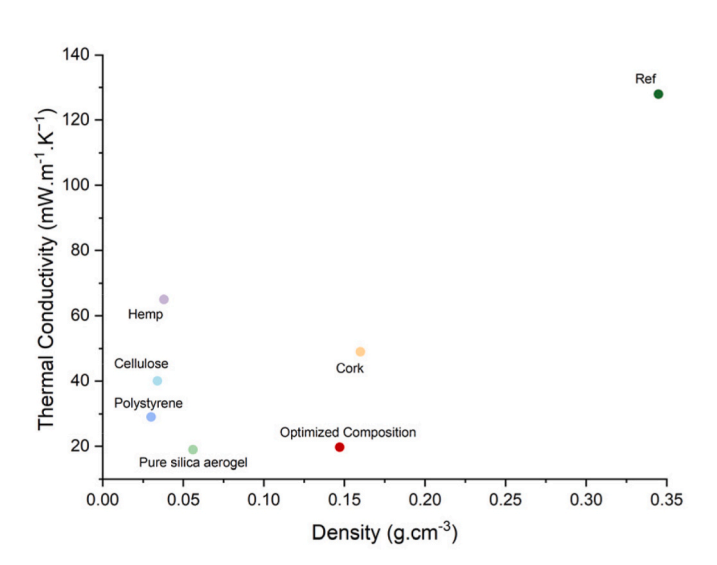


Fig. 9. Thermal conductivity of the different compositions: a) 1st Optimized compositions, b) 2nd Optimized compositions.



 $\textbf{Fig. 10.} \ \ \text{Density against thermal conducitivy}$

assess their structural integrity. Compression values will be compared to EN 13168, setting a 20 kPa threshold at 10 % strain, for insulating materials in the building sector. Results are displayed in Fig. 11.

Looking at the bio fillers, CI is the main material providing mechanical strength to the mix, with a compressive strength of 340 kPa,

way higher than the sawdust (82 kPa). This is mainly explained by the fiber length of loose cellulose, in addition to the good adhesion of the binder on the cellulose fiber, as seen in the micrographs in Fig. 12. Similar xanthan gum binding effect are observed for bio-based materials (Zhuang and Wang, 2025).

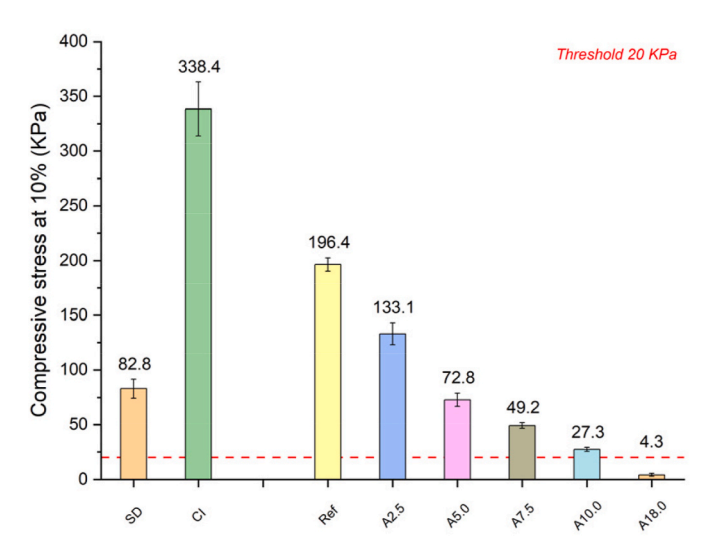


Fig. 11. Compressive stress value at 10 % displacement: Raw materials and early trials.

After adding brittle silica aerogel, an important drop is observed in the mechanical properties. The difference between the Ref. sample and the pure silica aerogel A18.0 is quite noticeable, with a decrease from 196 kPa to 4.3 kPa. However, adding bio fillers partially solves this problem, as all samples with silica aerogel (except A18.0) show a compressive strength above the 20 kPa threshold. This is explained by the good mixing of bio-fibers with the binder and silica aerogel particles, as shown in the micrographs in Fig. 13.

Then, compressive tests are performed on the optimized compositions, and the results are displayed in Fig. 14.

Results show that all samples remain above the 20 kPa threshold, with the lowest compressive stress value at 33.11 kPa. Their compressive behavior decreases as the quantity of cellulose decreases, which is responsible of the compressive strength (Fig. 10). All the samples with bio-based fillers fulfill the strength requirements for thermal insulation materials, even the ones with competitive thermal conductivity highlighted earlier.

3.4. Moisture behavior

3.4.1. DVS

DVS measurements are performed on several samples to assess the mass variation of the samples after exposure to relative humidities. Results are displayed in Fig. 15.

Among the components of the composite (Fig. 15 - a)), the binder's important hydrophilicity is highlighted, with a capacity of water absorption up to 120 % of its weight. On the contrary, silica aerogel particles absorb only 2 % of their weight by adsorption of moisture at the surface of the particles. This also explains the absence of hysteresis for silica aerogel, since no moisture is taken up by the sample. Commercial grade of silica aerogel are treated with hydrophobic treatment to prevent moisture sorption, due to their important sensitivity to moisture. Interestingly, the maximum moisture absorption of loose cellulose is about 20 % at the highest relative humidity, which is similar to that of other bio-based fibers, including barley straw (20 %) and wheat straw (23 %) (Koh et al., 2023). Looking at the composites (Fig. 15 - b)), the results are in the same range, between 55 % and 70 %, no matter the composition. The highest mass change for the composites is the composition made only of the binder and the silica aerogel (70 %). The effect of the binder on moisture sorption is highlighted as the main contributor to water sorption.

3.4.2. Impact on thermal conductivity

After being exposed to different relative humidities, the thermal conductivities of the samples are measured. Results for the different composites, at each relative humidity, are displayed in Fig. 16.

Looking at the gain in mass, the reduction of bio-fillers reduces the mass gain linked to moisture exposure, especially for the highest relative humidities. At 98 RH%, some samples exhibit some mold spots, therefore, it needs to be taken into account when considering the mass gain. Mold development, being a major drawback in bio-based materials, is

discussed later in this article. Moreover, looking at the thermal conductivity, a similar increase is observed among all the samples, and it does not differ when the quantity of silica aerogel changes. Among all the samples, a delta of $10-20~\text{mW}~\text{m}^{-1}.\text{K}^{-1}$ in thermal conductivity is observed between the dry condition and the highest relative humidity. The increase in thermal conductivity follows a linear function, typically observed for aerogel and bio-based materials (Hung et al., 2021), being the two types of materials in the mix.

3.4.3. Mold development

To investigate the mold development observed on some samples during the moisture uptake measurements, the samples are placed in 98 % RH for a month. Fig. 17 shows the surfaces of the different compositions.

The amount of mold differs in every sample, but two behaviors can be observed. Samples containing sawdust (SD and Ref.) showcase a larger amount of mold on their surface. On the other hand, the loose cellulose fiber (CI), treated with anti-fungi agent according to the supplier, seems to slow down or prevent mold development, but remains insufficient to full prevent the mold development. Sample A10.0 appears to be the composition with the best behaviour to mold development, with only a few spots of mold visible on the surface. Interestingly, the composition made without bio-fillers (A 18.0) also showcases mold development. Therefore, three Petri dishes are placed in a desiccator at high relative humidity: The first one contained raw sawdust, the second dried Xanthan Gum, and the third the binder (Xanthan Gum + Glycerol), all being exposed for the same period. Results are displayed in Fig. 18.

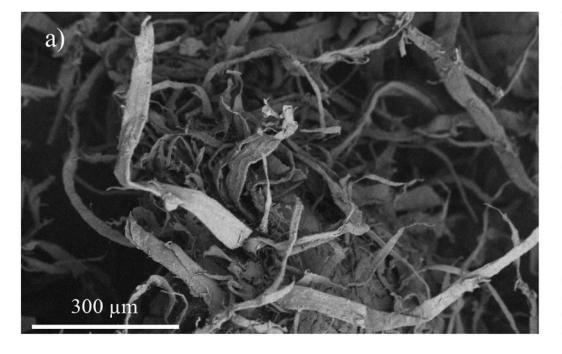
The results show the contribution of sawdust and wet binder (water + xanthan gum + glycerol) to the mold development. Yet, studied alone, xanthan gum does not promote mold dvelopement, therefore, most of the mold development is attribuated to the presence of glycerol. Due to its hydrophilicity (Roger et al., 1992), it promotes additional water in the system, creating perfect conditions for mold growing.

3.5. Flame retardancy test

The samples' half cuts after flame exposure (two times) are displayed in Fig. 19.

As the amount of bio-fillers decreases, the formed charcoal layer thickness decreases. From a silica aerogel amount of 7.5 wt% and above, the thickness remains the same. Interestingly, the composite without bio-fillers exhibits the thickest burnt layer, meaning that the bio-fillers act as fire protectant after short flame exposure. This phenomena could be explained by the formation of a char layer at the surface protecting the propagation of the flame throught the whole sample (Carosio et al., 2015). The total flame durations of the tested samples are displayed in Table 7, as well as the UL94 rating, assessing their flammability.

Based on the results, sawdust is the raw material that eases the duration and propagation of the flame the most. SD and Ref. Samples have a longer flame duration, above a minute, and cannot be re-ignited a



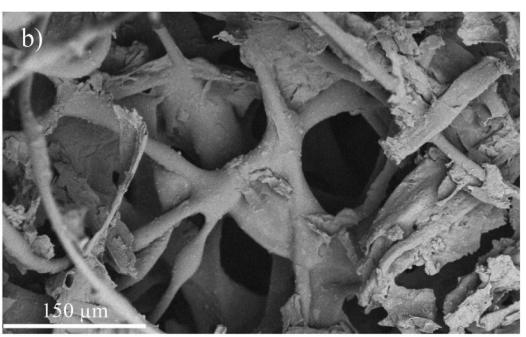


Fig. 12. SEM of Cellulose fibers: a) Pure cellulose (mag: x500) - b) Cellulose + Xanthan binder (mag: x940).

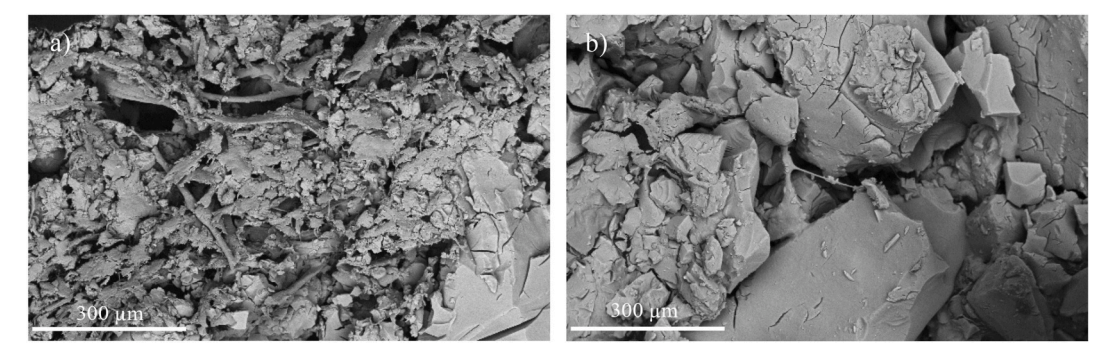


Fig. 13. SEM of Cellulose fibers: a) Sample A7.5 (mag: x500) - b) Sample A18.0 (mag: x500).

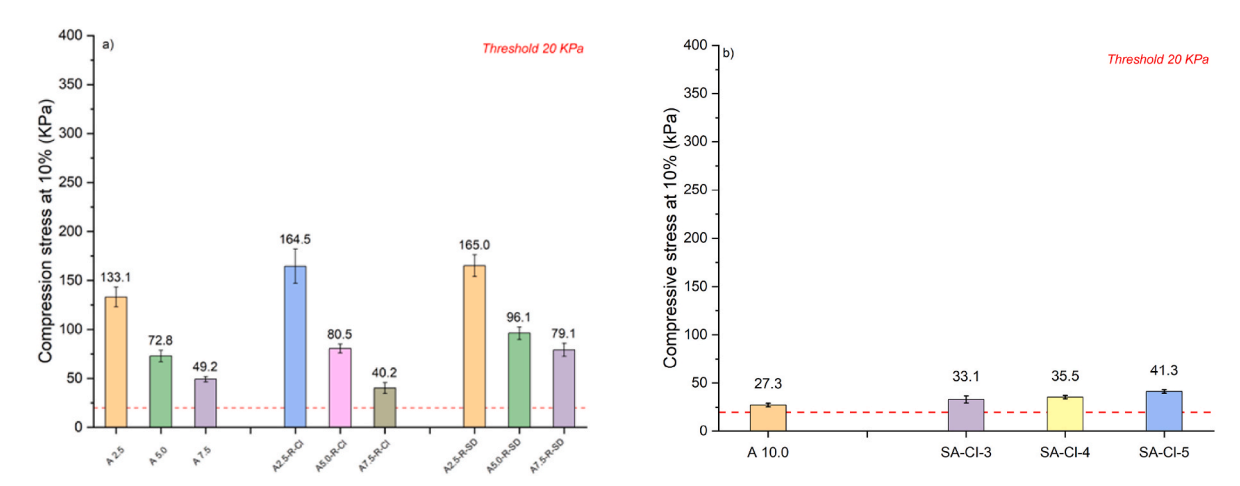
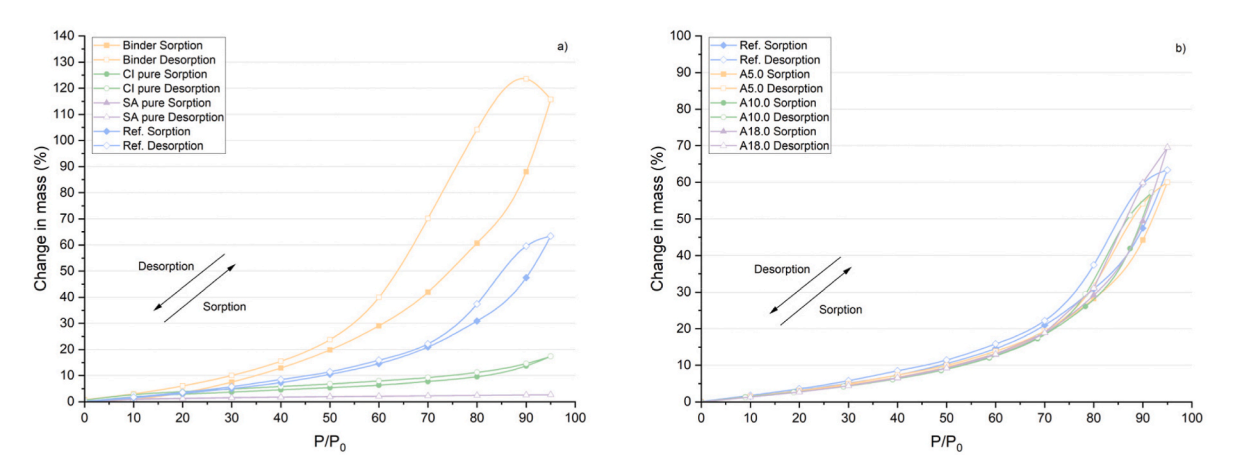


Fig. 14. Compressive stress values at 10 % displacement: a) 1st Optimized compositions, b) 2nd Optimized compositions.



 $\textbf{Fig. 15.} \ \ \textbf{Sorption isotherms: a) Single component, b) Composites.}$

second time. CI, treated with flame retardant according to the supplier, exhibits a shorter flame duration when tested alone, compared to SD and Ref., but remains unrated due to the long ignition time. Looking at the different composites containing silica aerogel, the flame duration decreases as the amount of silica aerogel increases, up to a minimum of approximately 10 s. A18.0, without any bio-fillers, burns for a slightly shorter time and could be classified with the highest resistance V-0, while the others can rank up at V-1 at best. This emphasizes the flame-retardant effect of silica aerogel. Most of the samples are rated at V-0 and V-1 and fulfill the minimum requirement for building applications.

4. Conclusions

This study focuses on the processing of silica aerogel composites with bio-waste-based binder and fillers, in order to assess the potential of the said composites as thermal insulation. Upon examining the findings, several key trends can be observed.

 Mixing silica aerogel with bio-based materials is feasible and results in building materials with competitive properties, compared to existing building materials for these applications.

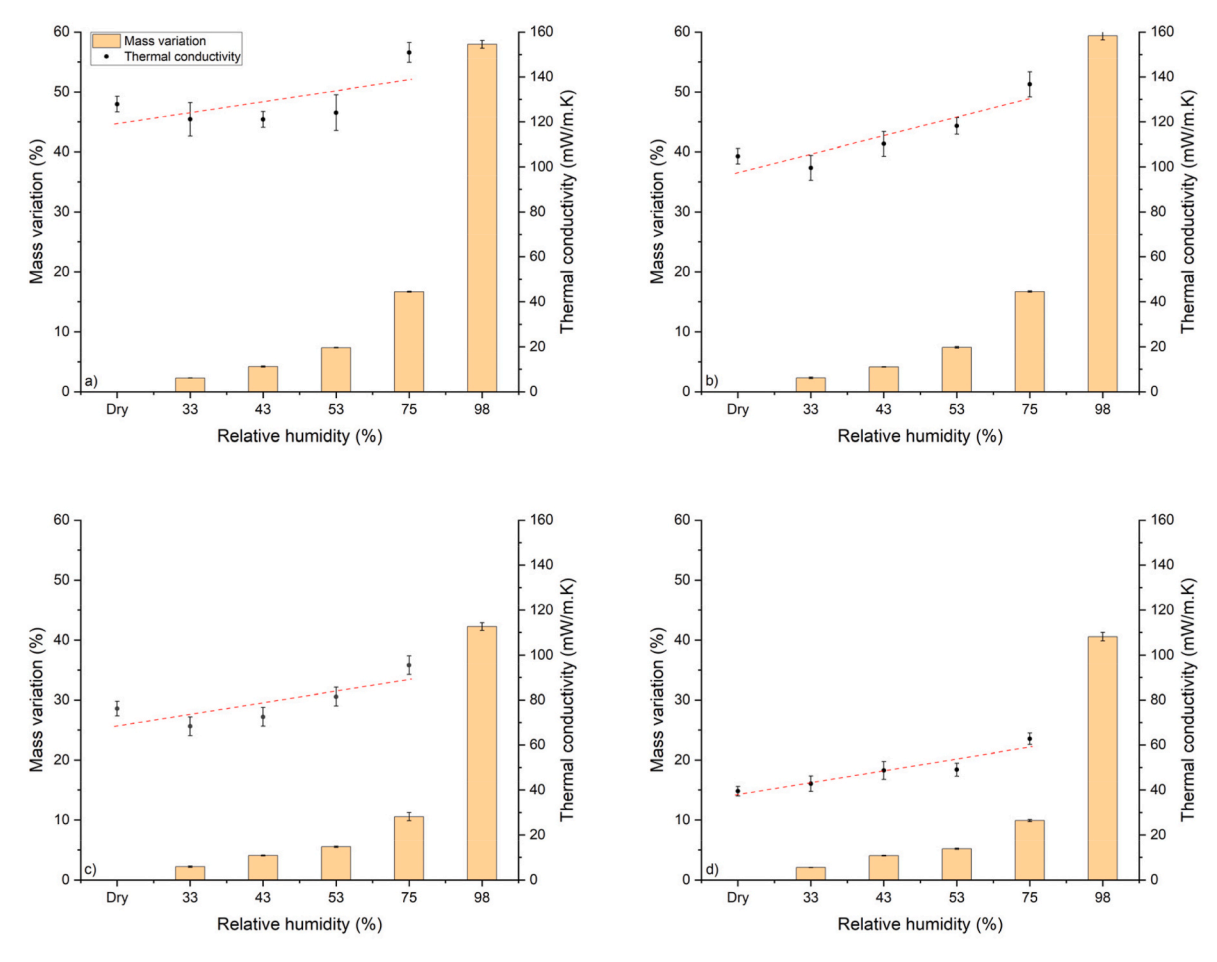


Fig. 16. Weight gain and thermal conductivity depending on the relative humidity: a) Ref. - b) A2.5 - c) A5.0 - d) A10.0.

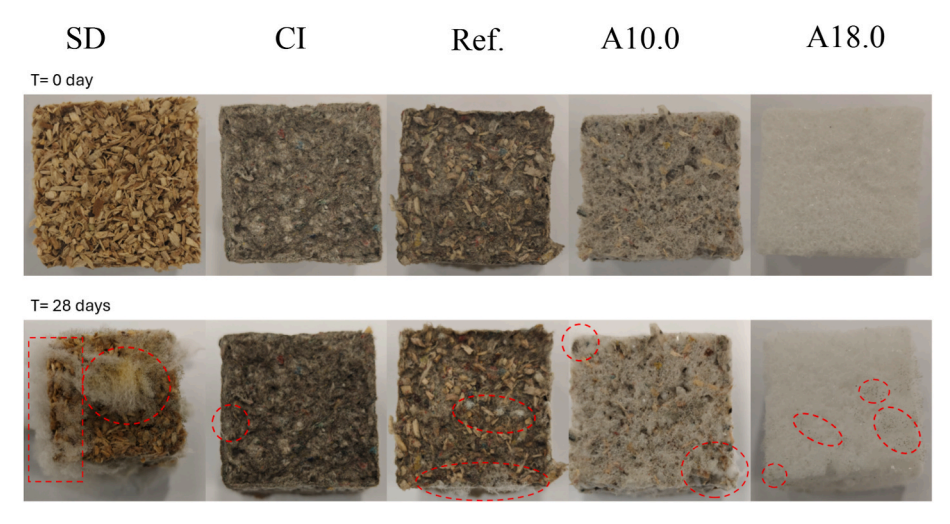


Fig. 17. Samples after 0 and 28 days, 98 %RH exposure.

- The role of the loose cellulose fiber is highlighted, and its coupling with xanthan gum and glycerol allows a fine-tuning of the properties due to excellent compatibilty,
- Designed materials have sufficient strength to meet the standard requirement for insulation materials, both with mechanical strength (>20 kPa) and flammability (grade V-0 or V-1).
- ullet As expected, increasing the quantity of silica aerogel leads to low thermal conductivity, with a minimal value of 19.7 mW m $^{-1}$.K $^{-1}$
- reached for the best mix, made with 72 wt% of binder, 3 wt% sawdust, and 15 wt% silica aerogel.
- The samples, like most bio-based materials, suffer from mold development at very high relative humidity. This could be addressed either by the addition of antifungals into the mix or by treatment of the bio-waste components before the processing.

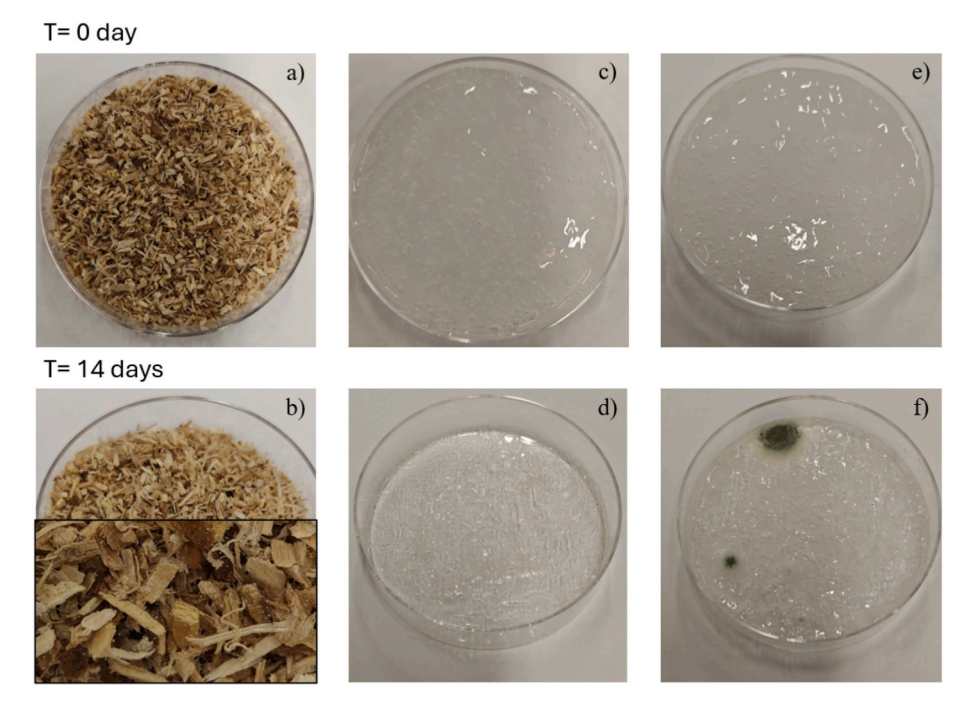


Fig. 18. 0 day and 14 days at 98 %RH exposure: a) and b): Pure sawdust, c) and d) Dried Xanthan gum, e) and f) Dried xanthan gum + glycerol.

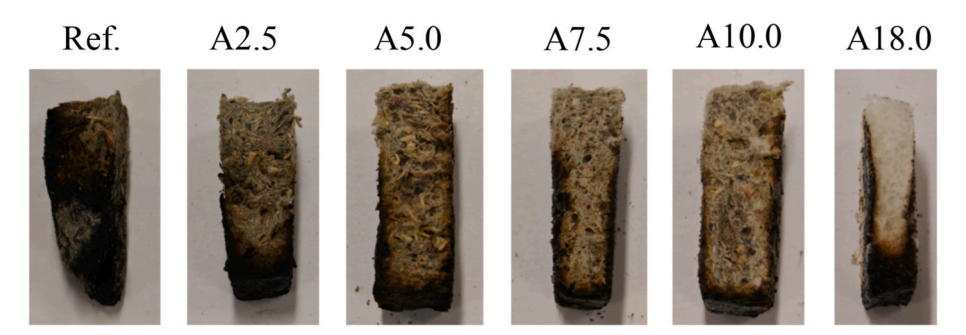


Fig. 19. Half-cut of samples after flame exposure.

Table 7 Flame duration of samples.

Sample	t ₁ (s)	t ₂ (s)	UL 94 rating
SD	$\textbf{75.7} \pm \textbf{21.9}$	N/A	Unrated
CI	40.3 ± 8.8	15.5 ± 1.5	Unrated
Ref.	91 ± 29.9	N/A	Unrated
A2.5	17.7 ± 2.5	15.5 ± 4.5	Unrated
A5.0	8.3 ± 3.1	12.7 ± 6.6	V-1
A7.5	6.0 ± 2.8	10.7 ± 6.6	V-1
A10.0	7.0 ± 4.2	6.0 ± 5.0	V-1
A18.0	4.3 ± 1.2	3.5 ± 1.5	V-0

CRediT authorship contribution statement

Samuel Pantaleo: Writing – original draft, Methodology, Investigation, Conceptualization. **Fenne Adriaanse:** Methodology, Investigation, Conceptualization. **Florent Gauvin:** Writing – review & editing, Supervision. **H.J.H. Brouwers:** Writing – review & editing, Supervision.

Declaration of competing interest

The authors declare that they have no known competing financial interests or personal relationships that could have appeared to influence the work reported in this paper.

Data availability

Data will be made available on request.

References

Benitez, J.J., et al., 2024. Transparent, plasticized cellulose-glycerol bioplastics for food packaging applications. Int. J. Biol. Macromol. 273, 132956. https://doi.org/10.1016/J.IJBIOMAC.2024.132956.

Berardi, U., Nosrati, R.H., 2018. Long-term thermal conductivity of aerogel-enhanced insulating materials under different laboratory aging conditions. Energy 147, 1188–1202. https://doi.org/10.1016/J.ENERGY.2018.01.053.

Bin Rashid, A., et al., 2023. Silica aerogel: synthesis, characterization, applications, and recent advancements. Part. Part. Syst. Char. 40 (6), 2200186. https://doi.org/10.1002/PPSC.202200186.

H. J. H. Brouwers. Y.X. Chen, K.M. Klima, K. Schollbach, Qingliang Yu, "Effect of Silica Aerogel on Thermal and Acoustic Insulation of Geopolymer Foam Concrete: towards the Role of Different Particle Sizesitle".

Carcassi, O.B., Minotti, P., Habert, G., Paoletti, I., Claude, S., Pittau, F., 2022. Carbon footprint assessment of a novel bio-based composite for building insulation. Sustainability 14, 1384. https://doi.org/10.3390/SU14031384 vol. 14, no. 3, p. 1384. https://doi.org/10.3390/SU14031384 vol. 14, no. 3, p.

Carosio, F., Fontaine, G., Alongi, J., Bourbigot, S., 2015. Starch-based layer by layer assembly: efficient and sustainable approach to cotton fire protection. ACS Appl. Mater. Interfaces 7 (22), 12158–12167. https://doi.org/10.1021/ACSAML5B02507/SUPPL_FILE/AM5B02507_SI_001.PDF.

Chen, W.H., Wang, C.W., Ong, H.C., Show, P.L., Hsieh, T.H., 2019. Torrefaction, pyrolysis and two-stage thermodegradation of hemicellulose, cellulose and lignin. Fuel 258, 116168. https://doi.org/10.1016/J.FUEL.2019.116168.

- Cosentino, L., Fernandes, J., Mateus, R., 2023. A review of natural bio-based insulation materials. Energies 16, 4676. https://doi.org/10.3390/EN16124676 vol. 16, no. 12, p. 4676, Jun. 2023.
- Demharter, A., 1998. Polyurethane rigid foam, a proven thermal insulating material for applications between $+130^{\circ}$ C and -196° C. Cryogenics 38 (1), 113–117. https://doi.org/10.1016/S0011-2275(97)00120-3.
- Faria, S., et al., 2011. Characterization of xanthan gum produced from sugar cane broth. Carbohydr. Polym. 86 (2), 469–476. https://doi.org/10.1016/J. CARBPOL.2011.04.063.
- Faruk, O., Bledzki, A.K., Fink, H.P., Sain, M., 2012. Biocomposites reinforced with natural fibers: 2000–2010. Prog. Polym. Sci. 37 (11), 1552–1596. https://doi.org/ 10.1016/J.PROGPOLYMSCI.2012.04.003.
- Grazieschi, G., Asdrubali, F., Thomas, G., 2021. Embodied energy and carbon of building insulating materials: a critical review. Cleaner Environ. Sys. 2, 100032. https://doi. org/10.1016/J.CESYS.2021.100032.
- Hung Anh, L.D., Pásztory, Z., 2021. An overview of factors influencing thermal conductivity of building insulation materials. J. Build. Eng. 44, 102604. https://doi. org/10.1016/J.JOBE.2021.102604.
- Iea. 2019 global Status Report for buildings and constructi on towards a zero-emissions, efficient and resilient buildings and constructi on sector [Online]. Available: www. iea.org. (Accessed 9 April 2025).
- Ijjada, N., Nayaka, R.R., 2022. Review on properties of some thermal insulating materials providing more comfort in the building. Mater. Today Proc. 58, 1354–1359. https://doi.org/10.1016/J.MATPR.2022.02.230.
- Koebel, M., Rigacci, A., Achard, P., 2012. Aerogel-based thermal superinsulation: an overview. J. Sol. Gel Sci. Technol. 63 (3), 315–339. https://doi.org/10.1007/ S10971-012-2792-9, 2012 63:3.
- Koebel, M.M., Wernery, J., Malfait, W.J., 2017. Energy in buildings—Policy, materials and solutions. MRS Energy Sustain. 4 (1). https://doi.org/10.1557/MRE.2017.14.
- Koh, C.H., Gauvin, F., Schollbach, K., Brouwers, H.J.H., 2022. Investigation of material characteristics and hygrothermal performances of different bio-based insulation composites. Constr. Build. Mater. 346, 128440. https://doi.org/10.1016/J. CONBUILDMAT.2022.128440.
- Koh, C.H., Gauvin, F., Schollbach, K., Brouwers, H.J.H., 2023. Upcycling wheat and barley straws into sustainable thermal insulation: assessment and treatment for durability. Resour. Conserv. Recycl. 198, 107161. https://doi.org/10.1016/J. RESCONREC.2023.107161.
- Kucharek, M., MacRae, W., Yang, L., 2020. Investigation of the effects of silica aerogel particles on thermal and mechanical properties of epoxy composites. Compos Part A Appl Sci Manuf 139, 106108. https://doi.org/10.1016/J. COMPOSITESA.2020.106108.
- Lin, P., Mah, M., Randi, J., DeFrances, S., Bernot, D., Talghader, J.J., 2023. High average power optical properties of silica aerogel thin film. Thin Solid Films 768, 139722. https://doi.org/10.1016/J.TSF.2023.139722.
- Liu, L., Wang, Z., Zhu, M., 2019a. Flame retardant, mechanical and thermal insulating properties of rigid polyurethane foam modified by nano zirconium amino-tris-(methylenephosphonate) and expandable graphite. Polym. Degrad. Stabil. 170, 108997. https://doi.org/10.1016/J.POLYMDEGRADSTAB.2019.108997.
- Liu, L., et al., 2019b. Experimental physical properties of an eco-friendly bio-insulation material based on wheat straw for buildings. Energy Build. 201, 19–36. https://doi. org/10.1016/J.ENBUILD.2019.07.037.
- Malfait, W.J., et al., 2024. The poor reliability of thermal conductivity data in the aerogel literature: a call to action. J. Sol. Gel Sci. Technol. 109 (2), 569–579. https://doi. org/10.1007/S10971-023-06282-9/FIGURES/5.

- Musco, A., Tarsi, G., Tataranni, P., Salzano, E., Sangiorgi, C., 2024. Use of bio-based products towards more sustainable road paving binders: a state-of-the-art review. J. Road Eng. 4 (2), 151–162. https://doi.org/10.1016/J.JRENG.2024.04.002.
- Parlato, M.C.M., Porto, S.M.C., Valenti, F., 2022. Assessment of sheep wool waste as new resource for green building elements. Build. Environ. 225, 109596. https://doi.org/ 10.1016/J.BUILDENV.2022.109596.
- Rech, A., et al., 2022. Waste-based biopolymer slurry for 3D printing targeting construction elements. Mater. Today Commun. 33, 104963. https://doi.org/ 10.1016/j.mtcomm.2022.104963.
- Roger, V., Fonty, G., Andre, C., Gouet, P., 1992. Effects of glycerol on the growth, adhesion, and cellulolytic activity of rumen cellulolytic bacteria and anaerobic fungi. Curr. Microbiol. 25 (4), 197–201. https://doi.org/10.1007/BF01570719/METRICS.
- Rong, M.Z., Zhang, M.Q., Ruan, W.H., 2013. "Surface modification of nanoscale fillers for improving properties of polymer nanocomposites: a review" 22 (7), 787–796. https://doi.org/10.1179/174328406X101247, 10.1179/174328406X101247.
- Sair, S., Mandili, B., Taqi, M., El Bouari, A., 2019. Development of a new eco-friendly composite material based on gypsum reinforced with a mixture of cork fibre and cardboard waste for building thermal insulation. Compos. Commun. 16, 20–24. https://doi.org/10.1016/J.COCO.2019.08.010.
- Sarkar, A., Islam, A., Zhu, L., Ren, S., 2024. Flame-retardant cellulose-aerogel composite from agriculture waste for building insulation. Appl. Mater. Today 36, 102080. https://doi.org/10.1016/J.APMT.2024.102080.
- F. Soghra Jahed, S. Hamidi, M. Zamani-Kalajahi, and M. Siahi-Shadbad, "Biomedical applications of silica-based aerogels: a comprehensive review," Macromol. Res., vol. 31, pp. 519–538, doi: 10.1007/s13233-023-00142-9.
- United Nations Environment Programme, 2022. 2021 global status report for buildings and construction: towards a zero-emission, efficient and resilient buildings and construction sector. Nairobi [Online]. Available: www.globalabc.org. (Accessed 3 May 2023).
- Wang, S., Li, H., Liu, L., 2024. Development of a multifunctional bio-based insulation material with corncob and silica aerogel. Energy Build. 323, 114817. https://doi. org/10.1016/J.ENBUILD.2024.114817.
- Xie, T., He, Y.L., Hu, Z.J., 2013. Theoretical study on thermal conductivities of silica aerogel composite insulating material. Int. J. Heat Mass Tran. 58 (1–2), 540–552. https://doi.org/10.1016/J.IJHEATMASSTRANSFER.2012.11.016.
- Yang, M., et al., 2023. Flexible electrospun strawberry-like structure SiO2 aerogel nanofibers for thermal insulation. Ceram. Int. 49 (6), 9165–9172. https://doi.org/ 10.1016/J.CFRAMINT.2022.11.076.
- Yu, Z.L., et al., 2018. Fire-retardant and thermally insulating phenolic-silica aerogels. Angew. Chem. Int. Ed. 57 (17), 4538–4542. https://doi.org/10.1002/
- Zhang, M., Resende, F.L.P., Moutsoglou, A., Raynie, D.E., 2012. Pyrolysis of lignin extracted from prairie cordgrass, aspen, and kraft lignin by Py-GC/MS and TGA/ FTIR. J. Anal. Appl. Pyrolysis 98, 65–71. https://doi.org/10.1016/J. JAAP.2012.05.009.
- Zhang, R., An, Z., Zhao, Y., Zhang, L., Zhou, P., 2020. Nanofibers reinforced silica aerogel composites having flexibility and ultra-low thermal conductivity. Int. J. Appl. Ceram. Technol. 17 (3), 1531–1539. https://doi.org/10.1111/JJAC.13457.
- Zhang, Z., Li, B., Wang, Z., Liu, W., Liu, X., 2023. Development of reduced thermal conductivity ductile cement-based composite material by using silica aerogel and silane. J. Build. Eng. 65, 105698. https://doi.org/10.1016/J.JOBE.2022.105698.
- Zhuang, Y., Wang, A., 2025. The mechanical properties and micro-mechanism of Xanthan Gum–Coconut shell fiber composite amended soil. Buildings 15, 1781. https://doi.org/10.3390/BUILDINGS15111781 vol. 15, no. 11, p. 1781, May 2025.